Photoinduced Electron-Transfer Reaction between the Erythrosin Dianion and $Mo(CN)_8^{4-}$ in the Presence of Various Cations. The First Example of Enthalpy−Entropy Compensation in Electron Transfer between Anions†

Edwin K. L. Yeow, Leonardo D. Slep, Alexander K. Chibisov,‡ and Silvia E. Braslavsky*

Max-Planck-Institut für Strahlenchemie, Postfach 10 13 65, D-45413 Mülheim an der Ruhr, Germany

Received: April 24, 2002; In Final Form: September 17, 2002

The electron-transfer reaction between the erythrosin dianion triplet, $^3Er^{2-}$, and $Mo(CN)_8^{4-}$ was studied by laser-induced optoacoustic spectroscopy in the presence of various cations (Li^+, Na^+, K^+, and Cs^+, all at 4.4 $\times 10^{-2}$ M analytical concentration). The buffer was in each case the corresponding $H_3BO_3/B(OH)_4^-$,M^+ (pH 9.18 at 20 °C). The enthalpy level of the triplet $^3Er^{2-}$ is $\Delta H_1 = 180 \pm 10$ kJ mol^{-1} independent of the cation. The structural volume change for $^3Er^{2-}$ formation is ΔV_1 = ca. 2 mL mol^{-1}, attributed to intrinsic changes upon its formation. The formation of the redox products $Er^{3-} + Mo(CN)_8^{3-}$ also leads to an expansion, ΔV_2, between 12 mL mol^{-1} for Li^+ and 8 mL mol^{-1} for Cs^+, which linearly correlates with the heat released during the radical formation step. The correlation is interpreted in terms of an enthalpy−entropy compensation effect, due to the strong influence of the cations on the H-bond water network, also reflected in the correlation between ΔV_2 and the literature values for the ability of the cations to organize the water structure. The entropic term for the formation of the free radicals upon triplet quenching thus originates in the water network rearrangement in the course of the electron-transfer process and is relatively large at room temperature.

Introduction

Electron-transfer reactions between molecules in solution and in biological systems (e.g., in redox proteins) are accompanied by changes in the structure of the reaction partners (internal changes) as well as by medium rearrangements, i.e., reorganization of the molecules that form the reaction cage. Internal changes result from variations in the reactants' bond lengths and angles, whereas medium changes, such as solvent reorganization, may be due to variations in the distribution of charges (electrostriction) and/or in specific solute−solvent interactions as a consequence of the electron-transfer reaction.

Laser-induced optoacoustic spectroscopy (LIOAS) is a convenient technique to determine the above-mentioned changes produced during photoinduced reactions. The time-resolved reaction enthalpy change ΔH_R and structural volume change ΔV_R (both quantities comprising the internal and medium rearrangements) can be readily determined with LIOAS.[1,2]

We recently found a linear correlation between ΔH_R and ΔV_R for the formation of the radical ion pair upon quenching of the metal-to-ligand charge-transfer triplet state (^{3}MLCT) of $Ru(bpy)_3^{2+}$ by the methyl viologen cation (MV^{2+}), along a series of added sodium salts. The strong linear dependence between the values of ΔH_R and ΔV_R was explained in terms of enthalpy−entropy compensation effects due to the perturbation of the H-bond network in water by the various anions.[3] In other words, the values of ΔH_R and ΔV_R were largely determined by the changes in the interactions of the reacting partners with the medium. The compensation effect was related to the anion effect on the $Ru(bpy)_3^{2+}$ emission-quenching rate by MV^{2+}.[4] Clark and Hoffman[4] found that both the forward and the backward electron-transfer rate constants within the solvent cage were strongly and similarly affected by the nature of the counterion.

In view of the fact that the Gibbs free energy ΔG_R of the reaction was constant throughout the series of anions,[4] the correlation ΔH_R vs ΔV_R determined by LIOAS led to the value of ΔG_R for the electron-transfer reaction. In fact, the intercept of the plot ΔH_R vs ΔV_R afforded the same ΔG_R value as measured.[3] Furthermore, the very large entropic term $T\Delta S_R$ in the Gibbs equation (comparable to the enthalpic term at room temperature), determined by the solvent rearrangement, documented the concept that entropy changes cannot be neglected in electron-transfer reactions.[3]

We argued that the above results were the consequence of changes in the structure of the water H-bond network due to perturbation by the counterion and that the H-bond network between the electron-transfer reaction partners controls the thermodynamics of the reaction.

Inasmuch as electron-transfer reactions in solution between partners of the same type of charge (i.e., both positive or both negative) should be mediated by the water H-bond network and the counterions, we decided to reanalyze[5] in light of the above findings the quenching reaction of the xanthene dye erythrosin triplet state ($^3Er^{2-}$) by a metal cyanide anion, $Mo(CN)_8^{4-}$, now in the presence of various monovalent cations. We chose this anion because in our previous work it showed the largest structural volume change among the various anions used, albeit a small value in absolute terms.[5] The buffer needed to avoid protonation and aggregation contained exclusively the corresponding cation.

We find in the present study a linear correlation between the values of ΔH and ΔV for the production of the radicals upon electron-transfer quenching of $^3Er^{2-}$ in the presence of Li^+, Na^+,

† Dedicated to Professor Karl Wieghardt on the occasion of his 60th birthday.

* To whom correspondence should be addressed. E-mail: braslavskys@mpi-muelheim.mpg.de. Fax: +49 (208) 306-3951.

‡ On leave from the Center of Photochemistry of the Russian Academy of Sciences, Novatorov St. 7a, 117421 Moscow, Russia.

10.1021/jp026006n CCC: $25.00
Published on Web 12/31/2002

K^+, or Cs^+ at identical concentrations. As ΔG of the reaction step can be assumed constant along the series of cations, the linear correlation leads again in this case to the value of ΔG for this particular step taking place in ca. 2 μs, provided that the intercept of the ΔH vs ΔV plot affords ΔG. However, for the production of the triplet state, we find no significant cation dependence for the ΔH and ΔV values.

Experimental Section

Materials. Erythrosin B (Iodeosin, Aldrich) was used as received. $K_4Mo(CN)_8 \cdot 2H_2O$ was prepared according to the literature procedure.[6] The potassium salt was converted into Li^+, Na^+, and Cs^+ salts by ion exchange chromatography. For consistency purposes, the same procedure was also applied for K^+. In a typical preparation, 1 mmol of $K_4Mo(CN)_8 \cdot 2H_2O$ was dissolved in 3 mL of Millipore-purified (Milli-Q) water and passed through a Dowex 50W X2 (200 mesh) cation exchange resin column ($l = 20$ cm, $d = 1.5$ cm) previously loaded with the desired counterion. The collected solution was then filtered through a 0.2 μm membrane and lyophilized to dryness (final pressure $<10^{-3}$ mbar), yielding a yellow fine powder of $M_4Mo(CN)_8 \cdot xH_2O$ ($x = 5$, 4, 2, and 2 for M = Li, Na, K, and Cs, respectively, according to elemental analysis).

To analyze the influence of the counterions on the photochemical and photophysical properties of the solutions, we used the Li^+, Na^+, K^+, or Cs^+ salt of $Mo(CN)_8^{4-}$ and $H_3BO_3/B(OH)_4^-$,M^+ buffer solutions with the same cation (in every case pH 9.18 at 20 °C). The individual buffers were prepared by mixing solutions of H_3BO_3 and M(OH) of the proper concentration, chosen to have the same concentration as that used in our previous study, i.e., 40 mM buffer, resulting in $[M^+] = 20$ mM.[5] The Na^+ concentration introduced by the erythrosin salt was negligible (7×10^{-6} M), i.e., more than 1000 times lower than the concentration of the added salt (6×10^{-3} M) and the buffer (20×10^{-3} M).

All solutions were bubbled for 10 min with argon prior to the fluorescence, LIOAS, and transient absorbance measurements.

Methods. Absorption spectra were recorded with a Shimadzu UV-2102PC spectrometer.

Steady-state fluorescence and excitation spectra were measured with a computer-controlled Spex-Fluorolog spectrofluorometer, as described by Aramendía et al.[7] Excitation at 510 nm was used to obtain the fluorescence spectra.

Flash photolysis with optical detection was performed with the equipment described by Schmidt et al.[8] Excitation was at 532 nm (second harmonic of a Nd:YAG laser, 15 ns pulses; JK Laser System 2000, Rugby, U.K.). The analyzing beam source was a pulsed Xe arc lamp for the detection at the short times, whereas it was a 100 W tungsten halogen lamp for the detection at the longer times. The temperature was 17 ± 1 °C.

For the LIOAS measurements, the method and equipment previously described were used.[1,5,9] The excitation source was the second harmonic (532 nm) of a Nd:YAG laser (Spectron Laser System, Rugby, U.K.; 8 ns pulses, repetition rate of 2 Hz). Absorbances of the erythrosin solutions ($A \approx 0.3$) were matched within 2% to those of the calorimetric reference bromocresol purple at the laser excitation wavelength. The concentration of $Mo(CN)_8^{4-}$ was chosen high enough (i.e., 6×10^{-3} M) to ensure ca. 80% quenching of $^3Er^{2-}$. Higher concentrations of the salts were not used to avoid salt-induced Er^{2-} aggregation, which would inhibit triplet-state formation.

The excitation beam was shaped by a 1.0 mm width slit which afforded an effective acoustic transit time of ca. 670 ns. A lifetime resolution of ca. 60 ns was therefore achieved by using deconvolution procedures. To avoid multiphotonic processes, the total energy of the laser pulse was <20 μJ, which lies within the linear fluence region for the system studied. The detecting system consisted of a 4 mm ceramic piezoelectric transducer (PZT, Vernitron), pressed against a cuvette's side wall parallel to the laser beam direction. The PZT signals were amplified 100 times (Comlinear E103, Ingolstadt), recorded by a digital oscilloscope (Tetronix TDS 684A), and transferred to a workstation and a PC for data analysis. An average of 100 acoustic waves were collected for the sample and calorimetric reference under the same conditions. The spectra remained essentially unchanged after the LIOAS experiments.

TABLE 1: Thermoelastic Parameter Ratio $c_p\rho/\beta$ for the 4×10^{-2} M $H_3BO_3/B(OH)_4^-$,M^+ Buffer Solutions with $M^+ = Li^+$, Na^+, K^+, or Cs^+

T, °C	$c_p\rho/\beta$, kJ mL^{-1}	T, °C	$c_p\rho/\beta$, kJ mL^{-1}	T, °C	$c_p\rho/\beta$, kJ mL^{-1}
12	33.4	20	19.4	35	11.8
14	27.6	25	15.7		
17	22.6	30	13.4		

The sample signal was considered as a convolution of the prompt instrument response function (measured with the calorimetric reference) and a time-dependent multiexponential decay function describing the pressure evolution in the sample. Deconvolution (using the Sound Analysis program, version 1.14, Quantum Northwest Inc., Spokane, WA) of the sample signal with the instrument response thus yielded the amplitude (φ_i) and lifetime (τ_i) values for the various decay processes. The several-temperatures method was employed between 12 and 35 °C.[1]

The thermoelastic parameter ratios $c_p\rho/\beta$ (Table 1; c_p = heat capacity, ρ = density, β = volume expansion coefficient) were determined for each buffer by comparing at each temperature the fluence-normalized LIOAS signal amplitude for bromocresol purple in water with that in the different buffer solutions. At each temperature the ratio $c_p\rho/\beta$ is essentially the same for the four cations (differences are less than 0.1%).

Results

The absorption spectra of erythrosin (7.2×10^{-6} M) in 40 mM $H_3BO_3/B(OH)_4^-$,K^+ buffer, of 1.2×10^{-2} M $K_4Mo(CN)_8$ in 40 mM $H_3BO_3/B(OH)_4^-$,K^+ buffer, and of the 1:1 mixture of both solutions are shown in Figure 1A.

The absorption spectra of the erythrosin solutions in 6×10^{-3} M solutions of the various $M_4Mo(CN)_8$ salts in the respective 40 mM $H_3BO_3/B(OH)_4^-$,M^+ buffer were very similar (Figure 1B). In particular, the visible absorption band was identical. There were some differences in the strength of the 400 nm shoulder, due to different absorption coefficients of the four $M_4Mo(CN)_8$ salts in this region.

The fluorescence spectra of the erythrosin solutions in the presence of the various $M_4Mo(CN)_8$ salts in $H_3BO_3/B(OH)_4^-$,M^+ buffer, excited at 510 nm (all A_{510} = ca. 0.2) were also very similar. All emission maxima were at 550 nm (Figure 1A), and the areas under the emission curves were also very similar, indicative of identical (within experimental error) fluorescence quantum yields.

The emission spectrum shape and its maximum were not changed upon dilution of the solutions containing each of the four cations, nor were the spectra changed upon decreasing the buffer concentration 10 times (spectra not shown). Upon buffer dilution, the relative emission quantum yield, as evaluated from the area under the emission curve, did not vary, strongly

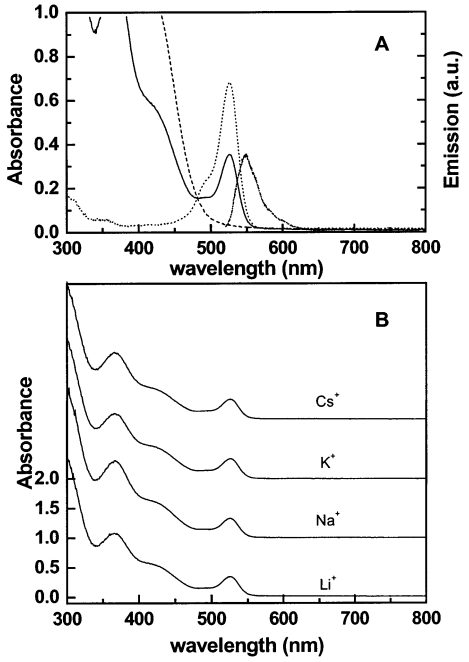

Figure 1. (A) Absorption spectrum of a (---) 7.2×10^{-6} M erythrosin solution in 4×10^{-2} M $H_3BO_3/B(OH)_4^-,K^+$ buffer, (— — —) 1.2×10^{-2} M $K_4Mo(CN)_8$ in 4×10^{-2} M $H_3BO_3/B(OH)_4^-,K^+$ buffer, and (—) a 1:1 mixture of the previous two. The emission spectrum (— - - —, $\lambda_{exc} = 510$ nm) of the latter solution is included. (B) Absorption spectra of 3.6×10^{-6} M solutions of erythrosin in the presence of 6×10^{-3} M $M_4Mo(CN)_8$ in 4×10^{-2} M $H_3BO_3/B(OH)_4^-,M^+$ buffer for $M^+ = Li^+$, Na^+, K^+, or Cs^+, all at pH 9.18 at 20 °C. The absorbance scale is only shown for the Li^+ spectrum. The other three are shifted for the purpose of comparison. In each case the spectra before and after the LIOAS experiments are shown; they are essentially identical.

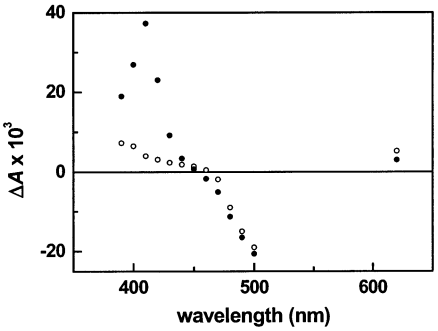

Figure 2. Transient absorption spectra after excitation with a 15 ns laser pulse at 532 nm of an erythrosin solution in 4×10^{-2} M $H_3BO_3/B(OH)_4^-,K^+$ buffer ($A_{532} = 0.302$, pH 9.18) (○) immediately after excitation and (●) 500 μs after excitation and in the presence of 6×10^{-3} M $K_4Mo(CN)_8$. $\lambda_{obs} = 410$ nm.

suggesting that aggregates of Er^{2-} are not formed at the buffer concentrations used. A higher buffer concentration would have produced aggregates known to inefficiently undergo intersystem crossing.

Transient absorbance spectra measured upon laser excitation at 532 nm of a solution of erythrosin in $H_3BO_3/B(OH)_4^-,K^+$ buffer in the absence and in the presence of $K_4Mo(CN)_8$ show that the triplet absorption of $^3Er^{2-}$ at 620 nm, observed immediately after excitation for the erythrosin solutions, was strongly quenched in the presence of $K_4Mo(CN)_8$ (Figure 2).

A new transient absorption at 410 nm indicative of the formation of the Er^{3-} radical was observed instead. The growth and decay of the 410 nm transient absorbance were monitored for erythrosin solutions in the presence of each of the four $M_4Mo(CN)_8$ salts (Figure 3). Three time windows were chosen, i.e., a 10 μs, a 20 μs, and a 10 ms window. The signals were measured as a function of the excitation pulse energy, and only the linear laser energy dependence region was used for the quantitative analysis.

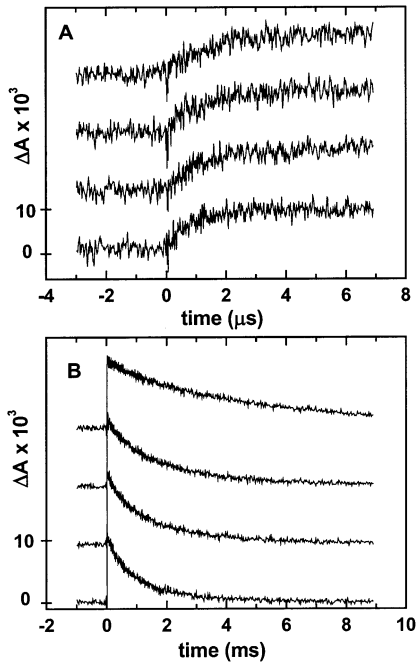

Figure 3. (A) Growth and (B) decay at 17 °C of the 410 nm transient absorption after excitation of erythrosin in the presence of 6×10^{-3} M $M_4Mo(CN)_8$ in 4×10^{-2} M $H_3BO_3/B(OH)_4^-,M^+$ buffer for M^+ (from top to bottom) = Li^+, Na^+, K^+, and Cs^+, all at similar (low) pulse energies. $A_{532} = 0.310$, 0.310, 0.302, and 0.315 for the solutions containing Li^+, Na^+, K^+, and Cs^+, respectively.

The erythrosin triplet ($^3Er^{2-}$) lifetime in degassed 4×10^{-2} M $H_3BO_3/B(OH)_4^-,K^+$ buffer ($A_{532} = 0.302$, pH 9.18) was 40 μs as measured from the 620 nm decay. For the Li^+-, Na^+-, and Cs^+-containing buffers the lifetimes were 20, 31, and 22 μs, respectively. Experiments with $[K_4Mo(CN)_8] = 1.05 \times 10^{-3}$, 1.50×10^{-3}, 3.00×10^{-3}, 5.26×10^{-3}, and 6.0×10^{-3} M showed kinetics for the absorbance decay at 620 nm due to $^3Er^{2-}$ identical to that for the 410 nm growth (Figure 3A) due to the free radical Er^{3-}. The same was observed in similar experiments with the Li^+, Na^+, and Cs^+ salts. The resulting quenching constants were $k_q = (7.1 \pm 0.4) \times 10^7$, $(6.1 \pm 0.2) \times 10^7$, $(6.3 \pm 0.2) \times 10^7$, and $(10 \pm 1) \times 10^7$ M^{-1} s^{-1} for Li^+, Na^+, K^+, and Cs^+, respectively. A value of $k_q = 1.9 \times 10^7$ M^{-1} s^{-1} (in Na^+-containing solutions at a higher ionic strength and recalculated for zero ionic strength) has been previously reported.[10]

After reaching an almost identical absorbance plateau, the kinetic traces of the 410 nm decay are cation dependent for the same quencher concentrations and laser energies (i.e., the same $[Er^{3-}]$) (Figure 3B). The ratio of the initial decay rates is 0.25:0.6:0.8:1 for Li^+, Na^+, K^+, and Cs^+, respectively (all data at 17 °C). The kinetics of the bulk recombination is complex, and more data would be needed to determine the second-order rate constants.

Extrapolation of the 410 nm decay lifetime in the 10 ms window, performed with signals within the linear part of the laser energy dependence (low excitation energies), led to an amplitude that turned out to be cation independent (Figure 4), confirming that the formation yield of the separated radicals (reaction 7; see the Discussion) is independent of the cation

TABLE 2: Values Obtained and Derived from the Plots (Figure 5) Following Eq 2[a]

	q_1,[b] kJ mol^{-1}	ΔH_1,[c] kJ mol^{-1}	ΔV_1,[d] mL mol^{-1}	$\Delta H_2 = q_2$,[e] kJ mol^{-1}	ΔV_2,[f] mL mol^{-1}	ΔH_R,[g] kJ mol^{-1}	ΔV_R,[h] mL mol^{-1}	ΔS^0_{str},[i] J K^{-1} mol^{-1}
Li^+	44.6	176	1.7	−31	11.9	145	13.6	−96
Na^+	42	179	2.2	−42	10.7	137	12.9	−16
K^+	37.2	184	1.9	−29	11.3	155	13.2	20
Cs^+	49	172	1.6	−48	8.1	124	9.7	34

[a] All values are per absorbed einstein, without consideration of the reaction quantum yield, which is equal in the four cases (Figure 4). [b] From plots in Figure 5: (intercept $\varphi_1)E_\lambda$. [c] $\Delta H_1 = (E_\lambda - q_1 - \Phi_f E_f)/\Phi_1$ (see the text).[5] [d] From plots in Figure 5: (slope $\varphi_1)E_\lambda$. [e] From plots in Figure 5: (intercept $\varphi_2)E_\lambda$. [f] From plots in Figure 5: (slope $\varphi_2)E_\lambda$. [g] $\Delta H_1 + \Delta H_2$. [h] $\Delta V_1 + \Delta V_2$. [i] From Marcus.[23]

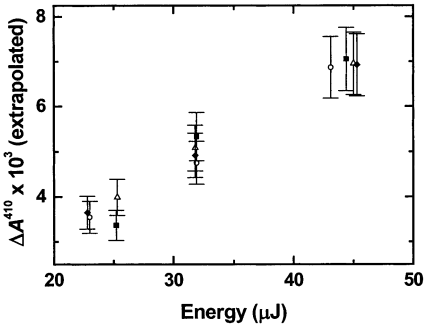

Figure 4. Laser pulse energy dependence of the absorbance at 410 nm after excitation of the solutions of erythrosin ($A_{532} = 0.310$, 0.310, 0.302, and 0.315 for the solutions containing (○) Li^+, (△) Na^+, (■) K^+, and (◆) Cs^+, respectively) in the presence of 6×10^{-3} M $M_4Mo(CN)_8$ salt and 4×10^{-2} M $H_3BO_3/B(OH)_4^-$,M^+ buffer of the M^+ as indicated. The extrapolation was from the decay in the 10 ms window (Figure 3B). The energy axis indicates the total laser pulse energy impinging on the cuvette.

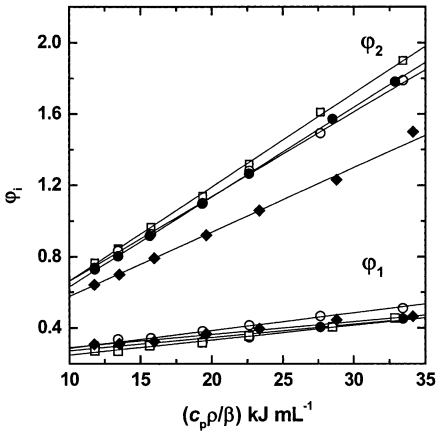

Figure 5. Preexponential terms vs the ratio of thermoelastic parameters $c_p\rho/\beta$ for the first (φ_1) and second (φ_2) terms of the biexponential function used for the convolution of the LIOAS signals (eq 2) after excitation (8 ns, 532 nm) of the Er^{2-} solutions in the presence of the respective $M_4Mo(CN)_8$ (6×10^{-3} M) and 4×10^{-2} M $H_3BO_3/B(OH)_4^-$,M^+ buffer (pH 9.18), (□) Li^+, (○) Na^+, (●) K^+, (◆) Cs^+. A_{532} was ca. 0.3 (the precise number depended on each solution), matched within 2% to the absorbance of the solution of bromocresol purple (used as a calorimetric reference) in the presence of the corresponding $M_4Mo(CN)_8$ and buffer. The temperature range is 12−35 °C.

present for the high quencher concentrations used. This is readily understood in view of the fact that the concentration of $Mo(CN)_8^{4-}$ (mostly ion paired; see the Discussion) was in every case large enough to make the product of the quenching constant $k_q = (6.3 \pm 0.2) \times 10^7$ M^{-1} s^{-1} times the quencher concentration larger than the nonquenched decay constant of $^3Er^{2-}$, i.e., $k_q[Mo(CN)_8^{4-}] =$ ca. 4×10^5 $s^{-1} > 1/\tau^3_{Er} = 0.25 \times 10^5$ s^{-1}. Therefore, the quantum yield of free radical formation approaches that of the intersystem crossing ($\Phi_R = \Phi_T$) provided that the geminate recombination is relatively less efficient than the escape rate of the redox products.

Convolution of the respective $H_3BO_3/B(OH)_4^-$,M^+ buffer/$M_4Mo(CN)_8$ solution of the calorimetric reference bromocresol purple with a double-exponential function describing the time evolution of the pressure pulse in the solution (eq 1)[1] gave excellent fitting of the sample LIOAS curve for each of the four erythrosin/$M_4Mo(CN)_8/H_3BO_3/B(OH)_4^-$,$M^+$ buffer solutions (fittings are not shown).

$$H(t) = \frac{\varphi_1}{\tau_1} e^{-t/\tau 1} + \frac{\varphi_2}{\tau_2} e^{-t/\tau 2} \qquad (1)$$

Taking into account that the amplitudes are a sum of the heat evolved and the structural volume change produced upon formation of the respective species (eq 2),[1−3] the intercept of

$$\varphi_i = \frac{q_i}{E_\lambda} + \frac{\Phi_i \Delta V_{str,i}}{E_\lambda}\left(\frac{c_p \rho}{\beta}\right)_T \qquad (2)$$

the plot of the reference-normalized amplitudes φ_i ($i = 1$ and 2) vs the thermoelastic parameter ratio for the respective solution at various temperatures, $(c_p\rho/\beta)_T$ (Figure 5), yields the values of the total heat evolved q_i and the slope yields the structural volume change per absorbed einstein, $\Delta V_{e,i} = \Phi_i \Delta V_{str,i}$, in each step i. Φ_i is the quantum yield and $\Delta V_{str,i}$ is the molar structural volume change corresponding to the respective process ($i = 1$ or 2). E_λ is the molar energy of the laser pulse. Table 2 contains the data for the four cations studied.

TABLE 3: Lifetimes for the Formation of Free Radical E^{3-} at $[Mo(CN)_8^{4-}] = 6 \times 10^{-3}$ M As Measured by LIOAS and Transient Absorbance (TA) at 410 nm, as Well as for the Decay of E^{3-} As Measured by TA at 410 nm[a]

	E^{3-} production[a] (LIOAS), $\mu s \pm 0.1$	E^{3-} production[b] (TA), $\mu s \pm 0.15$	E^{3-} decay[b] (TA), ms ± 0.1
Li^+	1.7	1.4	4
Na^+	1.3	1.65	1.5
K^+	1.4	1.2	1.2
Cs^+	0.9	0.8	1.0

[a] All data at 17 °C. Excitation was at 532 nm in all cases (8 ns pulses for LIOAS, 15 ns pulses for TA). [b] Average of three independent measurements. [c] Average of three values at the lowest energies employed.

The prompt ($i = 1$) component had in every case a lifetime ≤25 ns, whereas the second LIOAS-derived lifetimes were 1.7, 1.3, 1.4, and 0.9 μs at 17 °C for solutions containing Li^+, Na^+, K^+, and Cs^+, respectively. Similar values were obtained by monitoring at 620 nm the $^3Er^{2-}$ decay in the same solutions under the same conditions (Table 3).

To calculate ΔH_1 (Table 2), the energy lost by emission $\Phi_f E_f$ was taken into account in the energy balance, i.e., $\Delta H_1 = (E_\lambda - q_1 - \Phi_f E_f)/\Phi_1$.[5] The values of the fluorescence quantum yield of erythrosin ($\Phi_f = 0.02$ in aqueous solutions at pH 9)[11,12] and

SCHEME 1: Term Scheme Describing the Various Steps Analyzed and the Parameters Obtained[a]

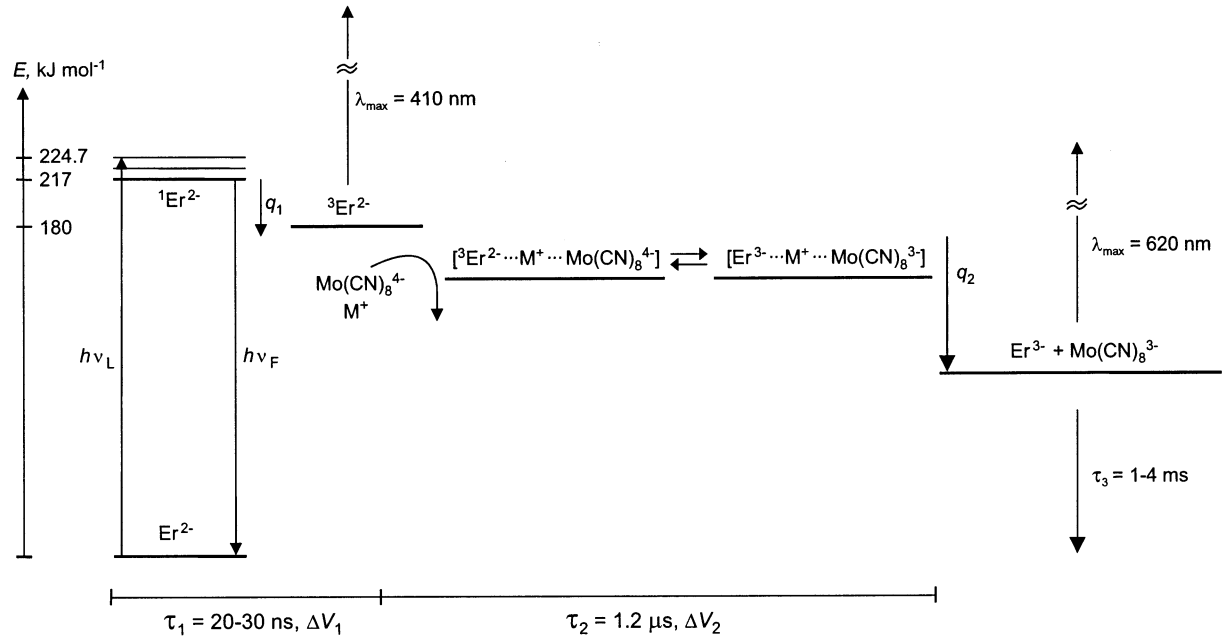

[a] In addition to the intermediate species, in which the cation is explicitly included, the reaction partners and products are also ion paired to variable degrees (see the text).

the average fluorescence energy $E_f = 217$ kJ mol^{-1} were identical in the presence of each of the four $M_4Mo(CN)_8$ salts.

The quantum yields for the formation of $^3Er^{2-}$ (the prompt process in LIOAS, up to reaction 4) Φ_1 were considered equal in the four cation solutions, because the quantum yield for the radical formation Φ_R is effectively the same in the four solutions, provided that the molar absorption coefficient of the radical species is the same in each of the various cation solutions (Figure 4) and reactions 4−7 (see the Discussion) are consecutive.

Discussion

The spectral position and shape of the lowest energy absorption band in the spectra of the solutions of erythrosin are the same in the presence of each of the four $M_4Mo(CN)_8$ salts in the respective $H_3BO_3/B(OH)_4^-$,M^+ buffer (Figure 1B) and are also identical to those of the respective band of erythrosin in buffer (Figure 1A). The position of the fluorescence maximum and the fluorescence yield (for excitation at 510 nm) are not perturbed either by the presence of the $M_4Mo(CN)_8$ salts. Thus, the excited-singlet-state energy level and lifetime (as judged from the constant fluorescence quantum yield) of erythrosin seem to be unperturbed by the salts. The same excited singlet state is populated and should be responsible for the fluorescence in all four cation solutions.

Taking into account the high $[M^+]$ when adding up that from the buffer (2×10^{-2} M) plus that from the quencher (4[quencher] $= 24 \times 10^{-3}$ M), the relative weight of ion pairing was calculated using the Fuoss equation[13] together with the radius of each of the ions involved. A radius of 3.31 ± 0.01 Å[14] from crystallographic data was taken for $Mo(CN)_8^{4-}$ and 7 ± 0.5 Å as a first approximation for the long axis of the elongated erythrosin (calculated from the rotational diffusional times measured for Er^{2-} in water at room temperature, 300−500 ps).[15] With these data it is calculated that 10% of the erythrosin ions are paired with the M^+ counterions whereas ca. 1% of the $H_3BO_3/B(OH)_4^-$ and 50% of the $Mo(CN)_8^{4-}$ are paired, with very little (if any) difference between the four cations.[3,4,16] Similar calculations lead to a ca. 25% ion pairing for $Mo(CN)_8^{3-}$ and 20% for Er^{3-}.

The prompt process with lifetime ≤25 ns observed for all four cations integrates all reactions leading to $^3Er^{2-}$ from free Er^{2-} (see Scheme 1). The small expansion (vide infra) observed for this step, ΔV_1 (Table 3), should thus be due to intrinsic changes upon triplet formation, similar to those found for the related compound rose bengal.[17]

The triplet state of erythrosin, $^3Er^{2-}$, produced with high efficiency (≥90% depending on the medium)[12,18] after excitation at 532 nm (reactions 3 and 4) and having a maximum differential absorption at 620 nm, is quenched by 6×10^{-3} M $M_4Mo(CN)_8$ salts as shown in Figure 2 for the case of K^+-containing erythrosin solutions. Within experimental error the quenching constant is roughly counterion independent, with the exception of Cs^+, with a constant higher than those of the other three.

As derived from the ion-pairing calculation, there is at least a 50% probability that, during the formation of the contact ion pair (reaction 5), one counterion will be involved during the encounter of the electron-transfer partners.

$$Er^{2-} + h\nu \rightarrow {}^1Er^{2-} \quad (3)$$

$$^1Er^{2-} \rightarrow {}^3Er^{2-} \quad (4)$$

$$^3Er^{2-} + [Mo(CN)_8^{4-}\cdots M^+] \leftrightarrows [^3Er^{2-}\cdots M^+\cdots Mo(CN)_8^{4-}] \quad (5)$$

$$[^3Er^{2-}\cdots M^+\cdots Mo(CN)_8^{4-}] \leftrightarrows {}^3[Er^{3-}\cdots M^+\cdots Mo(CN)_8^{3-}] \quad (6)$$

$$^3[Er^{3-}\cdots M^+\cdots Mo(CN)_8^{3-}] \rightarrow Er^{3-} + Mo(CN)_8^{3-} \quad (7)$$

Within the counterion-bridged ion pair $[^3Er^{2-}\cdots M^+\cdots Mo(CN)_8^{4-}]$, a thermodynamically favored electron transfer occurs which leads to the SSIRP $^3[Er^{3-}\cdots M^+\cdots Mo(CN)_8^{3-}]$ (reaction 6) in equilibrium with $[^3Er^{2-}\cdots M^+\cdots Mo(CN)_8^{4-}]$. The SSIRP then affords the free redox products Er^{3-} and $Mo(CN)_8^{3-}$ (reaction 7; see also Scheme 1). It is possible that these free radicals are also to some degree ion paired.

The process with lifetimes on the order of 1−2 μs (very similar in LIOAS and TA; see Table 3) corresponds to the

quenching of $^3Er^{2-}$, yielding the separated radicals (reactions 5−7). The lifetimes are identical for the decay of the triplet absorption at 620 nm and the growth of free radical formation at 410 nm. For the same conditions the lifetime is slightly shorter for the Cs^+-containing samples (Table 3).

The lifetimes obtained for the prompt reaction when the LIOAS signals were fitted with eq 1 were all ≤25 ns. The large slit used (1 mm, i.e., acoustic transit time of ca. 600 ns) did not allow a proper resolution of lifetimes in the tens of nanoseconds. Notwithstanding this fact, the amplitudes of the signal are a reliable measure of the integrated heat and structural volume change up to reaction 4.

The recombination of the separated radicals (reaction 8) occurs in the millisecond time domain as observed by transient absorbance (last column in Table 3, also with a lifetime determined by the countercation), being then too long with respect to the time window of the LIOAS experiments (maximum of ca. 10 μs); the separated redox free radicals are seen as final products in these experiments.

$$Er^{3-} + Mo(CN)_8^{3-} \rightarrow Er^{2-} + [Mo(CN)_8^{4-}\cdots M^+] \quad (8)$$

The use of eq 2 for the separation of the enthalpy and structural volume change contribution to each of the steps requires the knowledge of the reaction quantum yields as a function of the various cations.

The transient absorbance at 410 nm (corresponding to the free radical Er^{3-}) extrapolated from the 10 ms observation window (Figure 4) and plotted vs the laser excitation energy affords a plot independent of the cation at the lowest laser energies used, demonstrating that the formation yield of the separated radicals (reaction 7) is independent of the cation present. It is difficult to calculate absolute radical formation quantum yields in view of the strong overlapping of the absorbances of the various species involved.

Thermodynamic Parameters for the Formation of Triplet $^3Er^{2-}$. The intercepts and slopes of the plots in Figure 5 interpreted according to eq 2 (collected in Table 2) were used to calculate the enthalpy and structural volume changes for the formation of triplet $^3Er^{2-}$ and free redox products. The values in Table 2 are the structural volume and enthalpy changes per einstein of absorbed photons. Inasmuch as the quantum yield for the formation of the various species is constant along the series of cations, the values also represent the relative values per mole of produced species.

According to the assignment given above, $\Delta H_1 = 180 \pm 10$ kJ mol^{-1} is the energy content of the triplet state (per mole of produced species), independent of the counterion present within the error of the intercepts in Figure 5. The value of ΔH_1 is, within error, the same as the reported enthalpy content of $^3Er^{2-}$ (184 kJ mol^{-1}).[19]

The differences between the structural volume changes upon production of $^3Er^{2-}$ in the presence of the four counterions (a relatively small expansion of ca. 2 mL mol^{-1}, Table 2) are within experimental error, and the data do not correlate with the water-structuring properties of the cations, contrary to the ΔV_2 values (vide infra). Thus, we conclude that the structural volume changes for the processes leading to $^3Er^{2-}$ formation are determined by intrinsic changes. The energy level is only determined by the electronic properties of erythrosin and its transition (a $\pi\pi^*$ transition) and remains invariant (within experimental error) in the presence of the four cations.

Thermodynamic Parameters for the Formation of the Free Radicals upon Quenching of Triplet Erythrosin. The situation is different for the quenching of $^3Er^{2-}$. The kinetics

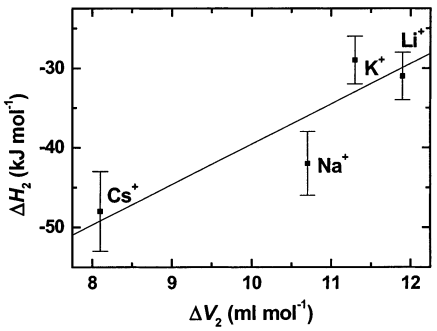

Figure 6. Enthalpy change ΔH_2 vs structural volume change ΔV_2 for the formation of the free redox products $Er^{3-} + [Mo(CN)_8^{3-}\cdots M^+]$ upon $^3Er^{2-}$ quenching by $[Mo(CN)_8^{4-}\cdots M^+]$ in buffer solution containing four counterions as indicated. The data were derived from LIOAS measurements. The temperature range of the measurements is 12−35 °C.

and quantum yield for the formation of the redox products are very similar for all four cations, although some deviation is observed for Cs^+. However, the values of the heat evolved $-q_2$ (eq 2; see Table 2) during the ca. 1.5 μs process of formation of $Er^{3-} + Mo(CN)_8^{3-}$ are cation dependent and correlate linearly with the values of the structural volume change for this process ΔV_2.

The plot of the enthalpy change for the formation of the redox products, i.e., $\Delta H_2 = -q_2$ vs the structural volume change for that process ΔV_2, from $^3Er^{2-}$ is shown in Figure 6.

In a manner similar to that found for the electron-transfer quenching of the ^{3}MLCT state of $Ru(bpy)_3^{2+}$ by the methyl viologen dication, MV^{2+}, in a series of monovalent anions, all at identical ionic strength, the values of the enthalpy and the structural volume change display a linear relationship in the series of different cations (Figure 6), empirically described by eq 9.[3]

$$\Delta H_2 = C + X\Delta V_2 \quad (9)$$

Taking into account that the ground-state spectra of erythrosin in all four cation solutions were unchanged, as well as the emission, and that the quantum yield for redox product formation was also invariant for the four cations, we consider that the free enthalpy for the formation of the free radicals ΔG_2 from $^3Er^{2-} + Mo(CN)_8^{4-}$ remains constant within the series. Unfortunately, the thermodynamic information on the system cannot be obtained by other means, e.g., by electrochemistry on the isolated redox couples, as erythrosin undergoes a concerted $2e^-/2H^+$ transfer on the electrode surface in aqueous solutions.[20]

In our previous study with $Ru(bpy)_3^{2+}$ and MV^{2+} in the presence of several anions, independent measurements showed that effectively $C = \Delta G$ for the formation of the free radicals.[3] Also, during our studies on sensory rhodopsin II[21] and on halorhodopsin, we could establish that, for the steps in which a $\Delta H - \Delta V$ compensation could be observed, the equations $X\Delta V = T\Delta S$ and, consequently, $C = \Delta G$ were valid, since the values determined for ΔS using these equalities agreed with previously calculated values of the entropy change (whenever available) for the corresponding reaction step.[22]

Thus, we assume that in the present case $C = \Delta G_2$ and thus $X\Delta V_2 = T\Delta S_2$ (eq 10).

$$\Delta H_2 = C + X\Delta V_2 = \Delta G_2 + T\Delta S_2 \quad (10)$$

Under the above assumption, $X = T\Delta S_2/\Delta V_2 = 5 \pm 2$ kJ mL^{-1} (slope of the plot in Figure 6).

Further support for the linear correlation between the structural volume change term and the entropic term in the Gibbs equation is the fact that the ΔV_2 values correlate with the tabulated entropy change due to the effect of the corresponding ions on the water structure, ΔS^0_{str} (Table 3).[23] The values of $\Delta S^0_{str} > 0$ are for structure-breaking ions, whereas those <0 are for structure-making ions. According to Marcus,[23] the value of ΔS^0_{str} between -30 and $+30$ should be taken with caution. In any case, it is just interesting to note the correlation, especially in the extremes (Li^+ vs Cs^+).

Again in this case we attribute the linear ΔH_2 vs ΔV_2 correlation to an enthalpy−entropy compensation effect,[24] determined by the changes in the water order introduced by the different cations. The compensation effect occurs during $^3Er^{2-}$ quenching, leading to the formation of the redox products. The value of ΔG_2 is assumed to remain constant, and with $C = \Delta G_2$, it is -90 ± 24 kJ mol^{-1} (intercept from the plot in Figure 6) for the formation of the redox products, whereas the values of ΔH_2 and ΔS_2 depend on the strong specific (hydrogen bond and ionic pairing) interactions of the partners with water. These interactions should involve the CN groups of the $Mo(CN)_8^{4-}$ complexes, as well as the polar groups in the erythrosin structure. Again in the present case, we find that the entropic term ($T\Delta S_2$) is large and is mainly determined by the water reorganization around the free radicals in the ion−radical pair. Under the assumption $C = \Delta G_2$, $T\Delta S_2 = 40-60$ kJ mol^{-1} (depending on the cation), i.e., of the same order as the enthalpic term (30−50 kJ mol^{-1}).

The value of ΔV_2 is in principle a sum of electrostrictive and specific effects. The fact that $\Delta V_2 > 0$ (from 12 to 8 mL mol^{-1}, Table 2) can be qualitatively explained by the enlargement of the solvation sphere between the separated radicals, most likely due to an enhanced Coulombic repulsion [$-3 \times -3 = 9$ vs $-2 \times -4 = 8$)].

It is possible to calculate the molar volume change due to electrostriction for the reaction from $Er^{2-} + Mo(CN)_8^{4-}$ to the free redox products $Er^{3-} + Mo(CN)_8^{3-}$ with the Drude−Nernst equation (11)[25] for each of the ions before and after electron

$$\Delta V_{el} = \frac{(ze)^2}{2r\epsilon}\frac{\partial(\ln \epsilon)}{\partial p} = -\frac{Bz^2}{r} \qquad (11)$$

transfer. z and r are the charge and radius of the ion in solution, respectively, ϵ is the dielectric constant, and $\partial(\ln \epsilon)/\partial p$ is its partial derivative with respect to pressure. In addition to the already mentioned radii of $Mo(CN)_8^{4-}$ and Er^{2-},[15] a value of 3.28 Å for the radius of $Mo(CN)_8^{3-}$, obtained from the X-ray structure, was used.[26] It was assumed that the variation upon formation of Er^{3-} is negligible.

Should the theoretical value of $B = 4.175$ mL Å mol^{-1} together with the above radii be used in eq 11, the values $\Delta V_{el} = 8.73$ mL mol^{-1} for the oxidation of $Mo(CN)_8^{4-/3-}$ and $\Delta V_{el} = -2.98$ mL mol^{-1} for the reduction of $Er^{2-/3-}$ would be obtained. The values add up to $\Delta V_{el} = 8.73 - 2.98 = 5.75$ mL mol^{-1} for the ground-state electron-transfer reaction, i.e., for

$$Er^{2-} + [Mo(CN)_8^{4-}\cdots M^+] \rightarrow\rightarrow\rightarrow Er^{3-} + Mo(CN)_8^{3-}$$

Thus, the calculated expansion is smaller than those derived from the measured values ($\Delta V_R = \Delta V_1 + \Delta V_2$, Table 3, and assuming a unity quantum yield for the formation of the free redox products) and certainly independent of the counterion. Using the semiempiric values calculated at 25 °C for B between 9.2 and 13.4 mL Å mol^{-1},[25] ΔV_{el} values between 13 and 18.5 mL mol^{-1}, respectively, are obtained. These values lie nearer those measured for ΔV_R (Table 3) although still independent of the counterion. The semiempiric B values already take into account possible interactions of the solutes with the surrounding water molecules. Thus, inasmuch as this calculation leads to figures similar to those measured, it is possible to state that in this case and upon use of the semiempiric B value, ΔV_{el} is similar to ΔV_R. As stated in a previous section the ΔV_1 values appear to be intrinsic to the triplet-state production of the ion-paired Er^{2-}, and in that case their origin should not be explained by electrostriction. However, they represent only 10% of the total volume change.

The cation dependence of the ΔV_2 values indicates a strong component from specific effects during this step. ΔV_2 and ΔH_2 are larger for the case of structure-making Li^+ since the number of hydrogen bonds affected is larger, whereas for the case of structure-breaking Cs^+, the number of hydrogen bonds involved is smaller.[24] This cation dependence is not taken into account by the semiempirical values of B.

A strong argument in favor of the participation of the countercation in the electron-transfer process is found in the fact that the bulk recombination of the free radicals is strongly cation dependent (Figure 3B). The bulk recombination can be represented as the sequence of steps 12−14, with k_1 and k_{-1} being the forward and backward reaction rate constants for the formation of the encounter complex and k_2 the electron-transfer rate constant within the encounter complex.

$$Er^{3-} + [Mo(CN)_8^{3-}\cdots M^+] \leftrightarrows [Er^{3-}\cdots M^+\cdots Mo(CN)_8^{3-}] \quad (k_1, k_{-1}) \qquad (12)$$

$$[Er^{3-}\cdots M^+\cdots Mo(CN)_8^{3-}] \rightarrow [Er^{2-}\cdots M^+\cdots Mo(CN)_8^{4-}] \quad (k_2) \qquad (13)$$

$$[Er^{2-}\cdots M^+\cdots Mo(CN)_8^{4-}] \rightarrow Er^{2-} + [Mo(CN)_8^{4-}\cdots M^+] \qquad (14)$$

Using the steady-state approximation, expression 15 is obtained for the observed bulk recombination rate constant of the free radicals.

$$k_{obs} = \frac{k_1}{1 + k_{-1}/k_2} \qquad (15)$$

As is apparent from Figure 3, $1/k_{obs}$ is the longest for Li^+ whereas it is the shortest for Cs^+. Hence, since it is reasonable to assume that k_1 and k_{-1} would be affected in a similar manner by the counterion, it should be the constant k_2 that increases in the order $Li^+ < Na^+ < K^+ < Cs^+$.

An alternative explanation for the cation dependence of the ΔV_2 values could be essayed on the basis of the speciation of the ion-pairing process. According to a very crude calculation using the Fuoss equation, there are more free cations after the electron-transfer process than in the ground-state parent compounds before light excitation. The percentage of cations set free upon photoinduced electron transfer is, in turn, slightly cation dependent. This could lead to cation-dependent ΔV_2 and ΔH_2 values. However, the observed compensation between the two values (Figure 6) reinforces our argument of the changes in the number and/or strength of hydrogen bonds between reactants and products with the water molecules during the electron-transfer reaction (the water structure changes along the cation series). The possible experiments to prove or disprove the alternative explanation imply working at higher ionic

strengths. As mentioned above, this is difficult because of the Er^{2-} aggregation at high ionic strengths.

Whatever the detailed mechanism is, it seems clear to us that it is the participation of the cation with its solvation sphere in the process of electron transfer that influences both the enthalpy and entropy of the quenching process.

The relatively long lifetime of the second component derived from the LIOAS data (ca. 1.3 μs for Na^+, Table 3) is the reason in our previous work this component was missed; i.e., the expansion of 1.9 mL mol^{-1} obtained using only the LIOAS amplitudes without deconvolution of the signals corresponds to the formation of $^3Er^{2-}$.[5] The calculation of the energy content of the species was done under the common assumption of no entropy change for the electron-transfer reaction, now known to be incorrect.

Acknowledgment. We gratefully acknowledge the able technical assistance of Andrea Keil-Block, Gudrun Klihm, and Dagmar Lenk, as well as the interesting discussions with Dr. Aba Losi. We are also indebted to Dr. Helmut Görner for valuable discussions and to Professor Wolfgang Lubitz for his support. L.D.S. was supported by a CONICET (Argentina) external fellowship.

References and Notes

(1) Gensch, T.; Viappiani, C.; Braslavsky, S. E. In *Encyclopedia of Spectroscopy and Spectrometry*; Tranter, G. E., Holmes, J. L., Eds.; Academic Press: San Diego, 1999; p 1124.

(2) Braslavsky, S. E.; Heibel, G. E. *Chem. Rev.* **1992**, *92*, 1381−1410.

(3) Borsarelli, C. D.; Braslavsky, S. E. *J. Phys. Chem. A* **1999**, *103*, 1719−1727.

(4) Clark, C. D.; Hoffman, M. Z. *J. Phys. Chem.* **1996**, *100*, 7526−7532.

(5) Habib-Jiwan, J.-L.; Chibisov, A. K.; Braslavsky, S. E. *J. Phys. Chem.* **1995**, *99*, 10246−10250.

(6) Heintz, E. A. *Inorg. Synth.* **1963**, *7*, 142−146.

(7) Aramendía, P. F.; Redmond, R. W.; Nonell, S.; Schuster, W.; Braslavsky, S. E.; Schaffner, K.; Vogel, E. *Photochem. Photobiol.* **1986**, *44*, 555−559.

(8) Schmidt, P.; Gensch, T.; Remberg, A.; Gärtner, W.; Braslavsky, S. E.; Schaffner, K. *Photochem. Photobiol.* **1998**, *68*, 755−762.

(9) Rohr, M.; Gärtner, W.; Schweitzer G.; Holzwarth, A. H.; Braslavsky, S. E. *J. Phys. Chem.* **1992**, *96*, 6055−6061.

(10) Zakharova, G. V.; Chibisov, A. K. *Khim. Fiz.* **1990**, *9*, 1311−1318.

(11) Bowers, P. G.; Porter, G. *Proc. R. Soc. London* **1967**, *A299*, 348−353.

(12) Wilkinson, F. *Organic Molecular Photophysics*; John Wiley & Sons: London, 1975; Vol. 2, Chapter 3.

(13) Fuoss, R. M. *J. Am. Chem. Soc.* **1958**, *80*, 5059−5061.

(14) (a) Leipoldt, J. G.; Basson, S. S.; Bok, L. D. C. *Inorg. Chim. Acta Lett.* **1980**, *44*, 99−101. (b) Nowicka, B.; Samotus, A.; Szklarzewicz, J.; Burgess, J.; Fawcett, J.; Russell, D. R. *Polyhedron* **1998**, *17*, 3167−3174. Basson, S. S.; Leipoldt, J. G.; van Wyk, A. J. *Acta Crystallogr., B* **1980**, *36*, 2025−2028.

(15) von Jena, A.; Lessing H. E. *Chem. Phys.* **1979**, *40*, 245−256.

(16) Clark, C. D.; Hoffman, M. Z. *J. Photochem. Photobiol., A* **1997**, *111*, 9−13.

(17) Gensch, T.; Braslavsky, S. E. *J. Phys. Chem. B* **1997**, *101*, 101−108, 3012.

(18) Lessing, H. E.; Richardt, D.; von Jena, A. *J. Mol. Struct.* **1982**, *84*, 281−292.

(19) (a) Nemoto, M.; Kokubun, H.; Koizumi, M. *Bull. Chem. Soc. Jpn.* **1969**, *42*, 1223−1230. (b) Kikuchi, K.; Kokubun, H.; Koizumi M. *Bull. Chem. Soc. Jpn.* **1970**, *43*, 2732−2739.

(20) Board, P. W.; Britz, D.; Holland, R. V. *Electrochim. Acta* **1968**, *13*, 1575−1579.

(21) Losi, A.; Wegener, A. A.; Engelhard, M.; Braslavsky, S. E. *J. Am. Chem. Soc.* **2001** *123*, 1766−1767.

(22) Losi, A.; Wegener, A. A.; Engelhard, M.; Braslavsky, S. E. *Photochem. Photobiol.* **2001**, *74*, 495−503.

(23) Marcus, Y. *Ion Solvation*; John Wiley Sons Ltd.: Chichester, U.K., 1985; p 125, Table 5.13.

(24) Grunwald, E. *Thermodynamics of Molecular Species*; John Wiley & Sons: New York, 1997; Chapter 6.

(25) Millero, F. J. *Chem. Rev.* **1971**, *71*, 147−176.

(26) Corden, B. J.; Cunningham, J. A.; Eisenberg, R. *Inorg. Chem.* **1970**, *9*, 356−362.